

Wright State University

CORE Scholar

[Browse all Theses and Dissertations](#)

[Theses and Dissertations](#)

2017

Linking the Variance of Permeability and Porosity to Newly Interpreted Lithofacies at the Site of the Illinois Basin - Decatur Project, Decatur, Illinois

Ritu Chaity Ghose
Wright State University

Follow this and additional works at: https://corescholar.libraries.wright.edu/etd_all



Part of the [Earth Sciences Commons](#), and the [Environmental Sciences Commons](#)

Repository Citation

Ghose, Ritu Chaity, "Linking the Variance of Permeability and Porosity to Newly Interpreted Lithofacies at the Site of the Illinois Basin - Decatur Project, Decatur, Illinois" (2017). *Browse all Theses and Dissertations*. 1769.

https://corescholar.libraries.wright.edu/etd_all/1769

This Thesis is brought to you for free and open access by the Theses and Dissertations at CORE Scholar. It has been accepted for inclusion in Browse all Theses and Dissertations by an authorized administrator of CORE Scholar. For more information, please contact library-corescholar@wright.edu.

LINKING THE VARIANCE OF
PERMEABILITY AND POROSITY TO
NEWLY INTERPRETED LITHOFACIES AT
THE SITE OF THE ILLINOIS BASIN –
DECATUR PROJECT, DECATUR,
ILLINOIS

Submitted in partial fulfillment
of the requirements for the degree of
Master of Science

By

RITU CHAITY GHOSE

B.S., University of Dhaka, 2014

2017

Wright State University

WRIGHT STATE UNIVERSITY

GRADUATE SCHOOL

Defense April 24, 2017

I HEREBY RECOMMEND THAT THE THESIS PREPARED UNDER MY SUPERVISION BY Ritu Chaity Ghose ENTITLED Linking the Variance of Permeability and Porosity to Newly Interpreted Lithofacies at the Site of the Illinois Basin - Decatur Project, Decatur, Illinois BE ACCEPTED IN PARTIAL FULFILLMENT OF THE REQUIREMENTS FOR THE DEGREE OF Master of Science.

Robert W. Ritzi, Ph.D.
Thesis Director

David F. Dominic, Ph.D.
Chair, Department of Earth &
Environmental Sciences

Committee on
Final Examination

Robert W. Ritzi, Ph.D.

David F. Dominic, Ph.D.

Doyle R. Watts, Ph.D.

Robert E. W. Fyffe, Ph.D.
Vice President for Research and
Dean of the Graduate School

Abstract

Ghose, Ritu Chaity. M.S. Department of Earth and Environmental Science, Wright State University, 2017. Linking the Variance of Permeability and Porosity to Newly Interpreted Lithofacies at the Site of the Illinois Basin - Decatur Project, Decatur, Illinois.

For effective geological sequestration of CO₂, it is critical to understand the processes associated with CO₂ movement and trapping in reservoirs, which requires a proper understanding of a diverse set of heterogeneous geologic properties. A highly-resolved data set from the Cambrian lower Mt. Simon sandstone reservoir (Unit A) in Decatur, Illinois, was used in a new approach to analyzing the variance of permeability and porosity. Newly interpreted bedding types, along with other factors, including grain size, and presence of bleached alterations, were considered in the analysis of variance. The results reveal that the factors contributing most to the sample variance in intrinsic permeability and porosity are variation in grain size and the presence or absence of bleaching. Grain size most explains the sample variance in intrinsic permeability in both horizontal and vertical directions, whereas bleaching most explains the sample variance in porosity and sample covariance between permeability and porosity. The contribution arising from differences in bedding type is very small. Interactions between factors were quantified and shown to be negligible.

Table of Contents

1. Introduction.....	01
2. New Interpretation of the Lower Mt. Simon Sandstone, Unit A	05
3. Methodology.....	12
4. Results.....	17
4.1 Analysis of $\hat{\sigma}_{YY}$ in data measured in horizontal directions	17
4.2 Analysis of $\hat{\sigma}_{YY}$ in data measured in the vertical direction	23
4.3 Analysis of $\hat{\sigma}_{\phi\phi}$	25
4.4 Analysis of $\hat{\sigma}_{Y\phi}$	27
5. Conclusion	29
6. References.....	31

List of Tables

Table 1: Summary statistics using composite data population	06
Table 2: Factors and categories used for partitioning the data into subpopulations	07
Table 3: Contribution to the (co)variance from the main factors and factor interactions	18
Table 4: Percent contribution to the (co)variance from the main factors and factor interactions.....	19
Table 5: Contribution to the (co)variance from the main factors in the hierarchical method.....	22
Table 6: Percent contribution to the (co)variance from the main factors in the hierarchical method.....	22
Table 7: Example of a parsimonious classification with four textural facies (Ritzi et al. 2016).....	30

List of Figures

Figure 1: Regional map of the Midwest region of the continental United States	.02
Figure 2: Wire-line log through the Lower Mt. Simon Sandstone Unit A03
Figure 3: Samples representing each grain size category08
Figure 4: Samples representing each bleaching category09
Figure 5: Samples representing each bedding category10
Figure 6: FMI log image for each bedding category11
Figure 7: Contributions from the main factors and interactions to $\ln(k_{hor_max})$.20
Figure 8: Contributions from the main factors and interactions to $\ln(k_{hor_min})$..20
Figure 9: Grain size and bedding type interaction for $\ln(k_{hor_max})$21
Figure 10: Grain size and bleaching interaction for $\ln(k_{hor_max})$21
Figure 11: Bedding and bleaching interaction for $\ln(k_{hor_max})$21
Figure 12: Contributions from the main factors and factor interactions to $\ln(k_{vert})$23
Figure 13: Grain size and bedding interaction for $\ln(k_{vert})$24
Figure 14: Grain size and bleaching interaction for $\ln(k_{vert})$24
Figure 15: Bedding and bleaching interaction for $\ln(k_{vert})$25
Figure 16: Contributions from the main factors and factor interactions to porosity26
Figure 17: Grain size and bedding interaction for porosity26
Figure 18: Grain size and bleaching interaction for porosity26
Figure 19: Bedding and bleaching interaction for porosity27
Figure 20: Contributions from the main factors and interactions to $\ln(k_{hor_max})$ & porosity covariance28
Figure 24: Conceptual model for 4 textural facies30

1. Introduction

An effective geological sequestration of CO₂ requires proper knowledge of the processes associated with CO₂ movement and trapping in reservoirs. The subsurface flow dynamics, which include CO₂ plume migration and the residual trapping of CO₂ within the reservoir, are controlled by a diverse set of sedimentary attributes. Heterogeneity is common. In a single rock unit sedimentary textures and structures, like grain size, bedding type, or bleaching alteration may vary over a range of scales, including small scales. The primary purpose of this study is to determine how these sedimentary textures and structures affect the variance of petrophysical properties like permeability or porosity of the reservoir rock. Because these properties may control plume behavior and storage of CO₂, understanding the variance in these properties is crucial (Gershenson et al., 2015).

The variance in permeability and porosity is here analyzed using a deterministic statistical approach (Isaaks and Srivastava, 1988). In deterministic statistics, sample statistics are calculated from a well-characterized dataset. The goal is to determine the factors that contribute to defining the value of a sample statistic. In this study, the focus is to understand how sedimentary attributes of a reservoir influence the sample variance for permeability and porosity.

The Cambrian lower Mt. Simon Sandstone CO₂ reservoir in Decatur, Illinois, was examined. In the Illinois Basin-Decatur Project (IBDP) one megaton of carbon dioxide was injected at a depth of 6561.68ft (2000m) into the lower Mt. Simon reservoir (Freiburg et al., 2014). This unit is separated from the Precambrian granite basement by a much less permeable series of sandstone and conglomerates referred to as the pre-Mt. Simon (Freiburg et al., 2014). The lower Mt. Simon is a reservoir with porosity generally above 10% and average permeability above 10 mD. This unit has been previously interpreted as mostly

fluvial braided river deposits (Freiburg et al., 2014). The lower Mt. Simon is further subdivided into two units: Unit A and Unit B. Unit A (357ft thick) is the lower unit (Freiburg et al., 2014). Unit A was the IBDP injection zone and is the focus of this study. Lithologically, it consists mostly of pinkish tan to maroon, friable, coarse to very fine grained sandstones, and pebble conglomerates (Freiburg et al., 2014). Bleached beds and spots are common. It is separated into upper and lower Unit A by a thin 2m thick mudstone, siltstone, and very fine grained sandstone facies. This low-permeability layer creates a pressure baffle between these two units. In this study I was interested in explaining the variation in permeability and porosity in the permeable units only and thus this mudstone layer is not included in this study.



Figure 1: Regional map of the Midwest region of the continental United States. The Illinois Basin is outlined and shaded in green; the location of the Illinois Basin - Decatur Project is labeled with a red star (Freiberg et al., 2014).

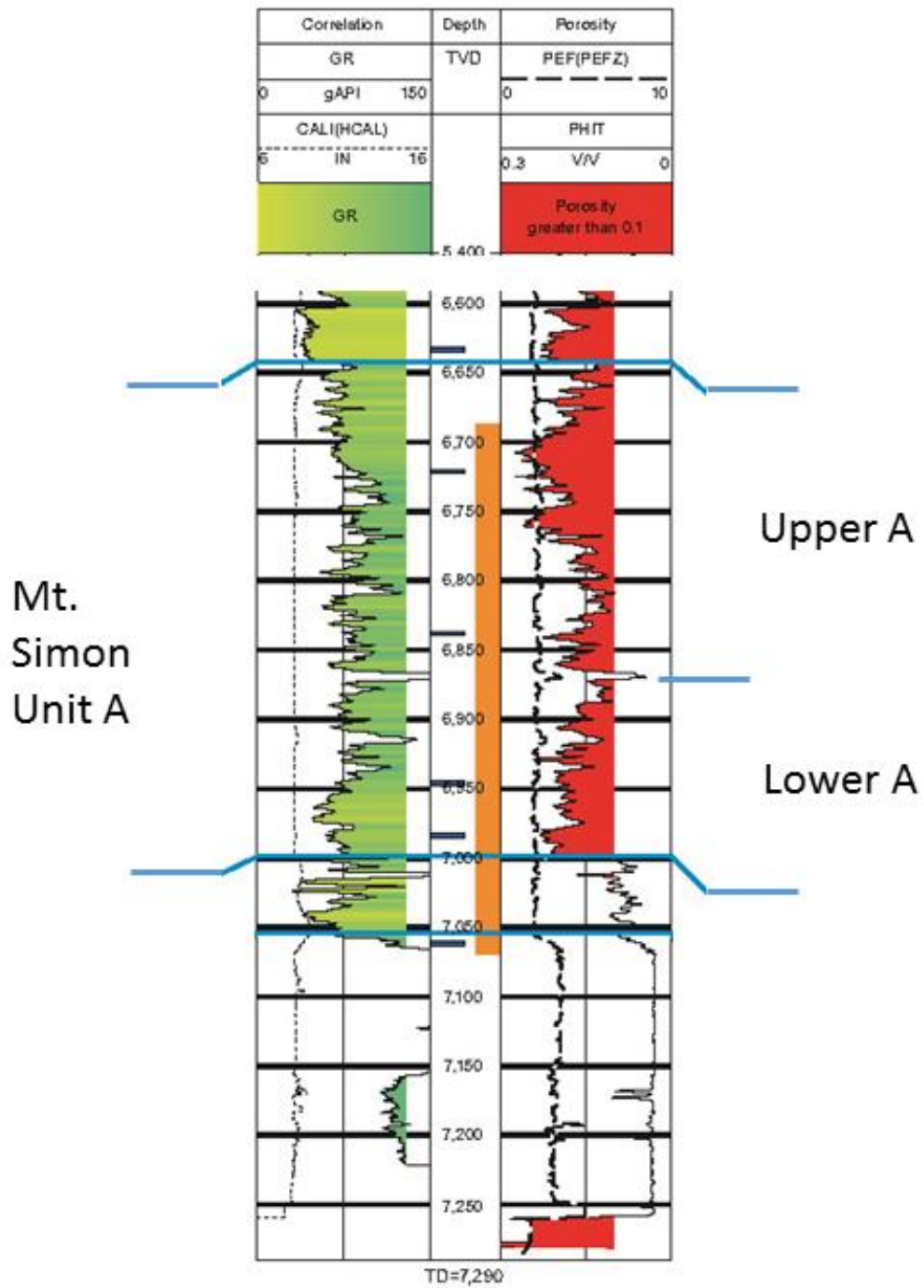


Figure 2: Wire-line log through the Middle Cambrian lower Mt. Simon Sandstone Unit A taken at the Illinois Basin-Decatur Project site (Freiburg et al., 2014). Porosity log on right is shaded red where exceeding 10%. Ochre stripe indicates interval of relatively continuous core sampling.

A verification well VW#1 is located 984.252ft (300m) from the injection well. Continuous core samples taken from VW#1 were used to create a highly-resolved dataset for sedimentary textures, permeability and porosity (Freiburg et al., 2014). Ritzi et al. (2016) used the highly-resolved data in an initial study linking the variance and covariance of porosity and permeability to sedimentary textures and structures. A new method for decomposing the sample variance and covariance was adapted for this purpose where indicator variables were used to represent a hierarchy of sedimentary attributes (Soltanian and Ritzi, 2014). Grain size, bedding type, bleaching alteration and vertical position were the four sedimentary attributes considered as possible controls on the variance of intrinsic permeability and porosity. Variation in grain size was the most important factor and had the biggest contribution to defining the sample variance of intrinsic permeability. The presence or absence of bleaching was the second most important contributor to the sample variance of permeability. The bleaching contribution was the most important contributor to the sample variance of porosity. The contributions arising from variation in bedding types and vertical position were negligible. Note that Ritzi et al. (2015) implicitly assumed that these factors influence the variance in permeability and porosity independently, and these factor interaction effects were negligible.

Recently the VW#1 core samples have been reexamined and the depositional environments and bedding structures of Freiberg et al. (2014) have been reinterpreted. The depositional environment of the lower Mt. Simon is no longer thought to be predominantly fluvial and new bedding structures have been identified. One goal of this study is to re-examine the variance in permeability and porosity and see to what extent the difference among the newly interpreted bedding structures is a contributing factor. Another goal of this study is to formally quantify and examine the effects of interactions between the main factors. In order to study the interactions, equations have been formulated to separate and quantify the effects arising from both the main factor effects and the interaction effects.

2. New Interpretation of the Lower Mt. Simon Sandstone, Unit A

The data used by Ritzi et al. (2016) come from the VW#1 core (Freiburg et al., 2014). Permeability and porosity are resolved with a 1ft (0.3m) spacing. Permeability was measured in the vertical direction and in two orthogonal horizontal directions, which are referred to as maximum and minimum horizontal k measurements (it is not known if these are the principal directions of k). Summary statistics are given in Table 1. The data have a large range in k , where k varies over more than three orders of magnitude, and thus a log transformation of the k values, $Y=\ln(k)$, is appropriate. The difference between the mean of maximum and minimum horizontal k is not very large and thus anisotropy is small within two orthogonal directions of measurement. However the anisotropy between horizontal and vertical k measurements are significant (6:1 or 5:1). Table 1 shows that porosity varies from 7% to 25% with an average porosity of 20%. Porosity (ϕ) varies within a small range and the need for log transformation is not indicated. The new bedding textures were not logged over the upper 4m included in Ritzi et al. (2016). Therefore the numbers of data in Table 1 are slightly lower and the statistics have small but negligible differences from those in Ritzi et al. (2016). Also some samples previously identified with bleach spotting were found to be more appropriately labelled as unbleached based on the disparity between the location of spotting and where permeability was measured in that section of core.

Table 1: Summary statistics using composite data population.

	Data	Ranges of value		Geometric mean (mD)	Variance	CV	Mean ln(k)	Variance ln(k)
		Max (mD)	Min (mD)					
Permeability								
$k_{hor\ max}$	219	498.86	0.12	30.1	4958.7	2.3	3.4	2.6
$k_{hor\ min}$	215	410.47	0.12	25.2	3313.9	2.3	3.2	2.6
k_{vert}	189	24.60	0.01	5.3	9233.9	18.3	1.7	8.8
Porosity	Data	Max (percent)	Min (percent)	Mean (percent)	Variance	CV		
	219	25	7	16	0.0014	0.2		

Table 2 lists the main factors and their categories that were considered as possible controls on the sample variance and covariance of permeability and porosity. The grain size and bedding factors are defined the same as in Ritzi et al. (2016). Fig. 3 shows examples of core samples for each of the five grain size categories. Fig. 4 shows core samples representing four bleaching categories. Bleached intervals are intervals that appear white-tan (Frieberg et al., 2014). There is greater porosity loss from compaction and cementation in bleached samples and bleaching reduces permeability by 75% (Ritzi et al., 2016). Bleaching may be caused by hydrocarbon invasion (Moulton 1926; Todd 1963; Levandowski et al., 1973; Dixon et al., 1989; Surdam et al., 1989), by hydrogen sulfide, by organic acids, by methane (Parry et al., 2004), or by Fe³⁺ reducing microbes (Roden 2008). The specific cause of bleaching in the lower Mt. Simon Sandstone is not known.

Table 2: Factors and categories used for partitioning the data into subpopulations.

Factors	Categories
Grain Size, r	Silt to Very Fine Sand, SVF
	Fine Sand, FS
	Medium Sand, MS
	Coarse Sand, CS
	Very Coarse Sand to Conglomerate, VC-CGL
Bedding Type, o	Crinkly Strata, CK
	Planar Bed, PB
	Cross Strata, CT
	Cross Laminae, CL
	Massive Bed, MB
Bleaching, j	Unbleached, UB
	Bleached Spot, BS
	Bleached Mottled, BM
	Bleached Bed, BB

Ritzi et al. (2016) showed that vertical position contributed very little to the variance of permeability and porosity. Therefore, vertical position is disregarded here. In Ritzi et al. (2016), data were subdivided into two bedding categories, i.e. cross bedded and non-cross bedded. In this analysis, instead of these two categories, five new bedding categories (Figure 5 and Table 2) have been used to subdivide the data. A new study has led to a revision in the interpretation of bedding structures, and the depositional environments they represent (Reesink and Best, personal communication). The FMI (micro-resistivity) log of the VW#1 core reveals bedding structures not readily apparent on freshly cut core samples. Figure 6 represents the FMI log images for each bedding type category corresponding to Figure 5.

The new categories include cross strata and cross laminae. Both refer to a unit of horizontal layers that are inclined at an angle to the main bedding plane. Cross laminae has layers less than 1cm thick, and cross strata have larger scales of stratification. Cross strata is the most common sedimentary structure and forms primarily by the migration of ripples or dunes. Cross strata and cross laminae account for more than 60% of the samples used for the analysis. Crinkly strata are irregularly-shaped, undular laminae with an amplitude ranging from 2 to 10 mm. They are common in fine to medium sand and often lined with silt, clay and micro-crystalline iron-oxides. Chips of the fine-grained laminae and a few potential roll-up structures were observed. 14% of the samples have this bedding structure. Planar strata refers to horizontal layering. Planar stratification can be formed under lower-stage or upper-stage flow conditions. 20% of the samples have planar bedding. Massive beds have little to no internal structure. Less than 1% samples have massive bedding.

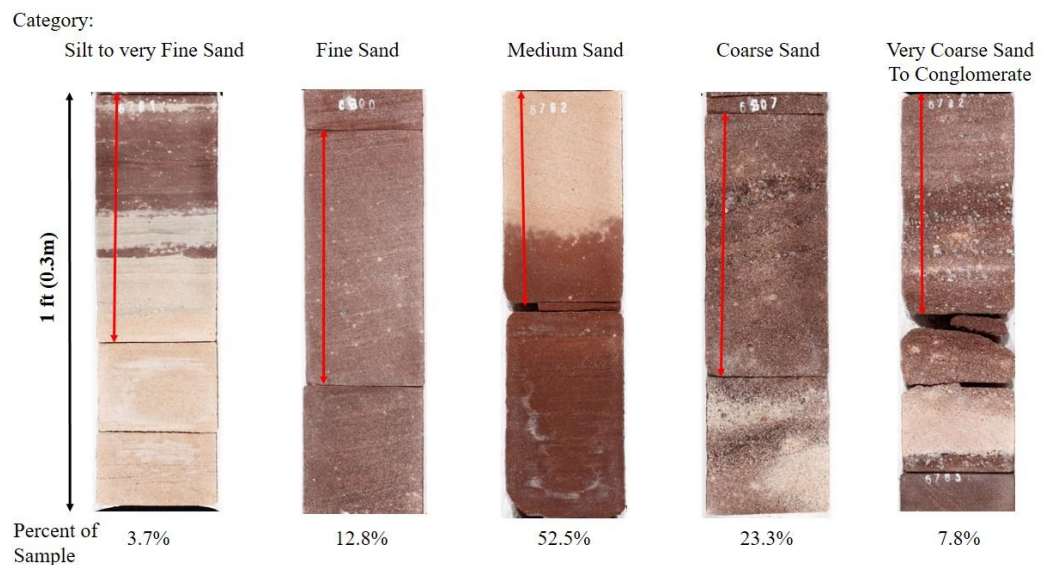


Figure 3: Samples from the lower Mt. Simon core VW1 representing each grain size category in Table 2. The red arrows indicate the piece used for measurement of intrinsic permeability. Samples from left to right: 1) Silt to Very-fine grained sandstone, $k_{hor\ max} = 0.63\ mD$, $k_{vert} =$ below detect, porosity = 9.80%, 6761-6761.60 ft depth. 2) Fine-grained sandstone, $k_{hor\ max} = 1.45\ mD$, $k_{vert} = 0.05\ mD$, porosity = 13%, 6800.10-6800.70 ft depth, 3) Medium-grained sandstone, $k_{hor\ max} = 12.31\ mD$, $k_{vert} = 1.85\ mD$, porosity = 19.20%,

6762-6762.55 ft depth, 4) Coarse-grained sandstone, $k_{hor\ max}= 69.66\text{mD}$, $k_{vert}= 69.21\text{ mD}$, porosity = 13.40%, 6807.1-6807.7 ft depth, 5) Very coarse-grained to Conglomerate, $k_{hor\ max}= 94.05\text{ mD}$, $k_{vert}= 17.28\text{ mD}$, porosity = 14.90%, 6782-6782.6ft depth.

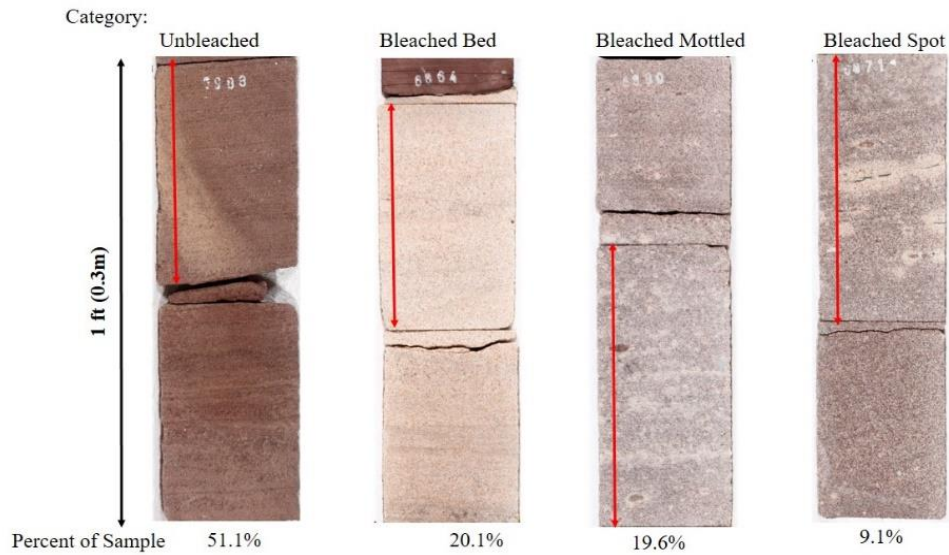


Figure 4: Samples from the lower Mt. Simon core VW1 representing each bleaching type category in Table 2. Samples from left to right: 1) Unbleached, $k_{hor\ max}= 121.37\text{mD}$, $k_{vert} = 11.34\text{mD}$, porosity = 21.4%, 6988.50-6989 ft depth. 2) Bleached bed, $k_{hor\ max}= 6.91\text{mD}$, $k_{vert}= 0.17\text{ mD}$, porosity = 12.30%, 6864.1-6864.6 ft depth 3) Bleached mottled, $k_{hor\ max}= 0.69\text{mD}$, $k_{vert}= 0.01$, Porosity = 7.50%, 6880.35-6881 ft depth, 4) Bleached spot, $k_{hor\ max}= 0.99\text{mD}$, $k_{vert} = \text{below detect}$, Porosity = 9.80%, 6871-6871.55 ft depth.

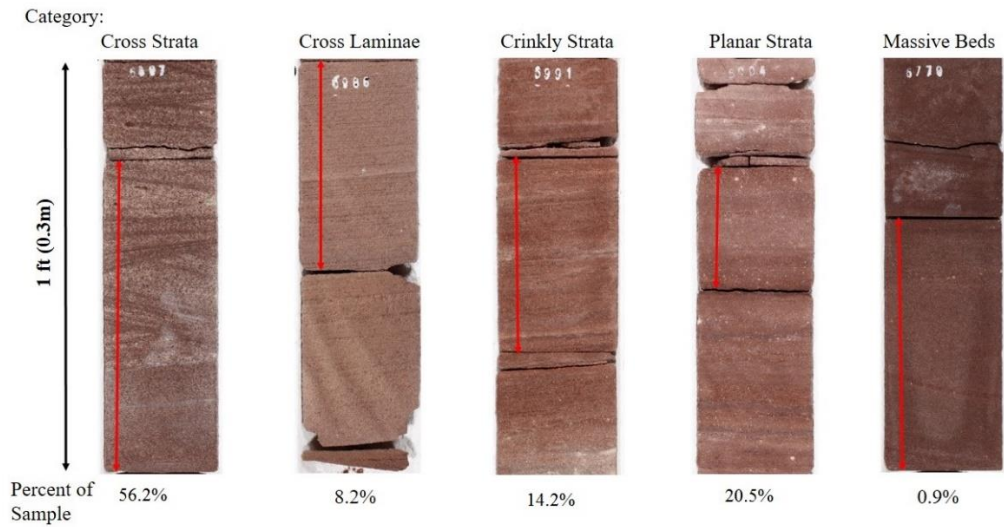


Figure 5: Samples from the lower Mt. Simon core VW1 representing each bedding type in Table 2. Samples from left to right: 1) Cross Strata, $k_{hor\ max}=66.51\text{mD}$, $k_{vert}=18.43\text{mD}$, porosity = 18.50%, 6897.25-6898 ft depth. 2) Cross Laminae, $k_{hor\ max}=151.31\text{mD}$, $k_{vert}=5.24\text{mD}$, Porosity = 20.50%, 6986-6986.50 ft depth, 3) Crinkly Strata, $k_{hor\ max}=211.65\text{mD}$, $k_{vert}=2.1\text{mD}$, Porosity = 19.50%, 6991.25-6991.70 ft depth, 4) Planar Strata, $k_{hor\ max}=15.3\text{mD}$, $k_{vert}=0.03\text{mD}$, Porosity = 14.20%, 6904.20-6904.90 ft depth, 5) Massive, $k_{hor\ max}=22.59\text{mD}$, $k_{vert}=21.06\text{mD}$, Porosity=17.4%, 6779.40-6780 ft depth.

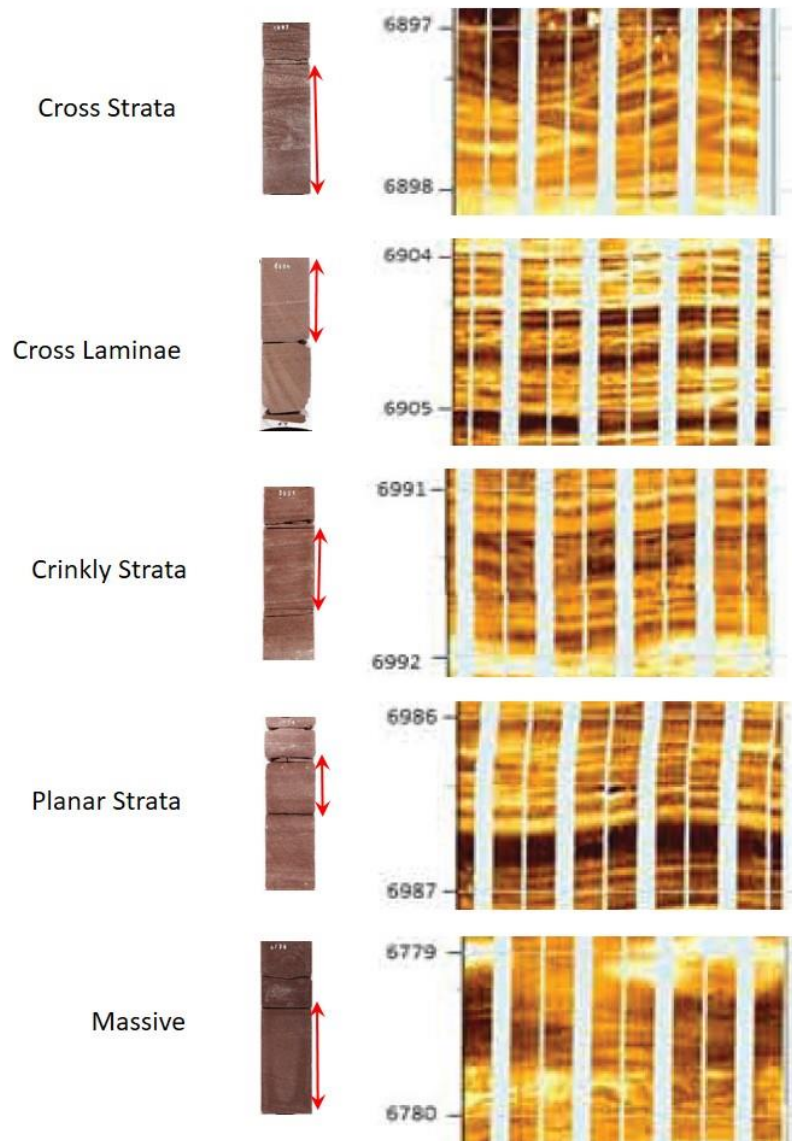


Figure 6: FMI log image for each bedding category in Figure 5.

3. Methodology

Let $\xi(i)$ be a sample of an attribute such as Y or ϕ . The data were subdivided into subpopulations based on the three different factors and their categories. If defined as in Ritzi et al. (2016) then the subpopulations are defined hierarchically with subset ξ_r containing samples that belong to the grain size category 'r', [r = SVF, FS, MS, CS, VC-CGL], ξ_{ro} containing samples in category 'r' and within bedding type category 'o', [o = CK, PB, CT, CL, MB], and ξ_{roj} containing samples within category 'r', 'o' and the bleaching category 'j' [j = UB, BS, BM, BB].

The next step was to define an integer indicator variable for each sample that tracks the factor categories corresponding to the sample. The indicator variable for the grain size category is I_r , and the value of I_r is 1 when the sample is within 'r' category, and otherwise 0. Similarly, the value of I_{ro} is 1 when sample belongs to 'o' category within 'r' category, and otherwise 0 and I_{roj} is 1 when sample comes from within category 'r' within category 'o' within category 'j', and otherwise 0.

The sample proportions were calculated for the Ritzi et al. (2016) hierarchy using following equations:

$$\hat{P}_{roj} = \frac{1}{N_t} \sum_{i=1}^{N_t} I_{roj}(i) = \frac{N_{roj}}{N_t} \quad (1)$$

$$\hat{P}_{ro} = \frac{1}{N_t} \sum_{i=1}^{N_t} I_{ro}(i) = \frac{N_{ro}}{N_t} \quad (2)$$

$$\hat{P}_r = \frac{1}{N_t} \sum_{i=1}^{N_t} I_r(i) = \frac{N_r}{N_t} \quad (3)$$

Sample means were determined by:

$$\hat{m}_{\xi_{roj}} = \frac{1}{N_{roj}} \sum_{i=1}^{N_{roj}} \xi_{roj}(i) \quad (4)$$

$$\hat{m}_{\xi_{ro}} = \frac{1}{N_{ro}} \sum_{i=1}^{N_{ro}} \xi_{ro}(i) = \sum_j \hat{m}_{\xi_{roj}} \frac{\hat{P}_{roj}}{\hat{P}_{ro}} \quad (5)$$

$$\hat{m}_{\xi_r} = \frac{1}{N_r} \sum_{i=1}^{N_r} \xi_r(i) = \sum_o \hat{m}_{\xi_{ro}} \frac{\hat{P}_{ro}}{\hat{P}_r} = \sum_j \hat{m}_{\xi_{rj}} \frac{\hat{P}_{rj}}{\hat{P}_r} \quad (6)$$

$$\hat{m}_{\xi} = \frac{1}{N_t} \sum_{i=1}^{N_t} \xi(i) = \sum_{r=1}^{N_r} \hat{m}_{\xi_r} \hat{P}_r = \sum_{o=1}^{N_o} \hat{m}_{\xi_o} \hat{P}_o = \sum_{j=1}^{N_j} \hat{m}_{\xi_j} \hat{P}_j \quad (7)$$

Here, to separate the main factor effects from factor interactions, the data are also divided according to other possible subpopulations, and the mean of those populations are defined as:

$$\hat{m}_{\xi_{rj}} = \frac{1}{N_{rj}} \sum_{i=1}^{N_{rj}} \xi_{rj}(i) = \sum_j \hat{m}_{\xi_{roj}} \frac{\hat{P}_{roj}}{\hat{P}_{rj}} \quad (8)$$

$$\hat{m}_{\xi_{oj}} = \frac{1}{N_{oj}} \sum_{i=1}^{N_{oj}} \xi_{oj}(i) = \sum_j \hat{m}_{\xi_{roj}} \frac{\hat{P}_{roj}}{\hat{P}_{oj}} \quad (9)$$

$$\hat{m}_{\xi_o} = \frac{1}{N_o} \sum_{i=1}^{N_o} \xi_o(i) = \sum_o \hat{m}_{\xi_{ro}} \frac{\hat{P}_{ro}}{\hat{P}_o} = \sum_j \hat{m}_{\xi_{rj}} \frac{\hat{P}_{oj}}{\hat{P}_o} \quad (10)$$

$$\hat{m}_{\xi_j} = \frac{1}{N_j} \sum_{i=1}^{N_j} \xi_j(i) = \sum_j \hat{m}_{\xi_{rj}} \frac{\hat{P}_{rj}}{\hat{P}_j} = \sum_j \hat{m}_{\xi_{oj}} \frac{\hat{P}_{oj}}{\hat{P}_j} \quad (11)$$

The sample variance is given by:

$$\hat{\sigma}_{\xi\xi}^2 = \frac{1}{N_t} \sum_{i=1}^{N_t} (\xi(i) - \hat{m}_\xi)^2 \quad (12)$$

The sample variance was decomposed into sums of squares which quantify the contributions of the main factors and the interactions (Kutner et al., 2005):

$$\hat{\sigma}_{\xi\xi}^2 = SS_r + SS_o + SS_j + SS_{ro} + SS_{rj} + SS_{oj} + SS_{roj} + SS_\varepsilon \quad (13)$$

Where the main factor effects are:

$$SS_r = \sum_r (\hat{m}_{\xi_r} - \hat{m}_\xi)^2 \hat{P}_r = \sum_r \hat{m}_{\xi_r}^2 \hat{P}_r - \hat{m}_\xi^2 \quad (14)$$

(15)

$$SS_o = \sum_o (\hat{m}_{\xi_o} - \hat{m}_\xi)^2 \hat{P}_o = \sum_o \hat{m}_{\xi_o}^2 \hat{P}_o - \hat{m}_\xi^2$$

$$SS_j = \sum_j (\hat{m}_{\xi_j} - \hat{m}_\xi)^2 \hat{P}_j = \sum_j \hat{m}_{\xi_j}^2 \hat{P}_j - \hat{m}_\xi^2$$

(16)

and the factor interaction effects are:

$$SS_{ro} = \sum_r \sum_o \hat{m}_{\xi_{ro}}^2 \hat{P}_{ro} - \sum_r \hat{m}_{\xi_r}^2 \hat{P}_r - \sum_o \hat{m}_{\xi_o}^2 \hat{P}_o + \hat{m}_\xi^2$$

(17)

$$SS_{rj} = \sum_r \sum_j \hat{m}_{\xi_{rj}}^2 \hat{P}_{rj} - \sum_r \hat{m}_{\xi_r}^2 \hat{P}_r - \sum_j \hat{m}_{\xi_j}^2 \hat{P}_j + \hat{m}_\xi^2$$

(18)

$$SS_{oj} = \sum_o \sum_j \hat{m}_{\xi_{oj}}^2 \hat{P}_{oj} - \sum_o \hat{m}_{\xi_o}^2 \hat{P}_o - \sum_j \hat{m}_{\xi_j}^2 \hat{P}_j + \hat{m}_\xi^2 \quad (19)$$

$$\begin{aligned}
SS_{roj} = & \sum_r \sum_o \sum_j \hat{m}_{\xi_{roj}}^2 \hat{P}_{roj} - \sum_r \sum_o \hat{m}_{\xi_{ro}}^2 \hat{P}_{ro} - \sum_r \sum_j \hat{m}_{\xi_{rj}}^2 \hat{P}_{rj} - \sum_o \sum_j \hat{m}_{\xi_{oj}}^2 \hat{P}_{oj} \\
& + \sum_r \hat{m}_{\xi_r}^2 \hat{P}_r + \sum_j \hat{m}_{\xi_j}^2 \hat{P}_j + \sum_o \hat{m}_{\xi_o}^2 \hat{P}_o - \hat{m}_{\xi}^2
\end{aligned} \tag{20}$$

and:

$$SS\varepsilon = \sum_r \sum_o \sum_j \hat{\sigma}_{\xi\xi_{roj}}^2 P_{roj} \tag{21}$$

Here SS_r , SS_o and SS_j terms represent the main factor effects from grain size, bedding types and bleaching respectively. SS_{ro} is the combined effect or the factor interaction effect from the grain size and bedding type. SS_{rj} and SS_{oj} are factor interactions arising from the grain size-bleaching and bedding type-bleaching respectively. SS_{roj} is the interaction effect coming from all of these three factors. $SS\varepsilon$ is the effect due to base level variability, i.e. the variance not explained and quantified or accounted for by the factors defined here. Note that order of the subscripts does not matter. For example subpopulation ξ_{ro} is the same as subpopulation ξ_{or} . Given that is true, and all interactions are accounted for, there is no hierarchy to the definition of subpopulations or the way the variance was decomposed.

The hierarchical decomposition by Ritzi et al. (2016) followed a different derivation which leads to the decomposition terms:

$$\hat{\sigma}_{\xi\xi}^2 = \alpha + \beta + \chi + \varepsilon \tag{22}$$

Where,

$$\alpha = \sum_r \hat{m}_{\xi_r}^2 \hat{P}_r - \hat{m}_{\xi}^2 \tag{23}$$

$$\beta = \sum_r \sum_o \hat{m}_{\xi_{ro}}^2 \hat{P}_{ro} - \sum_r \hat{m}_{\xi_r}^2 \hat{P}_r \tag{24}$$

$$\chi = \sum_r \sum_o \sum_j \hat{m}_{\xi_{roj}}^2 \hat{P}_{roj} - \sum_r \sum_o \hat{m}_{\xi_{ro}}^2 \hat{P}_{ro} \tag{25}$$

$$\varepsilon = \sum_r \sum_o \sum_j \hat{\sigma}_{\xi_{roj} \xi_{roj}} \hat{P}_{roj} \quad (26)$$

Here, the α term gives the contribution to the sample variance that comes from the sample mean differences from five grain size categories. This term is equivalent to the term SS_r from the first analysis because this is at the top of their hierarchy. The β term gives the contribution that arises from the contrast of sample means among the bedding type categories and the interaction between the grain size and the bedding factors. This term is equivalent to the sum of SS_o and SS_{ro} . The χ term denotes the contribution coming from the contrast in sample means among the four bleaching categories and the interactions between it and the other two factors separately and together. χ is equivalent to $SS_j + SS_{rj} + SS_{oj} + SS_{roj}$. The ε term gives the contribution that is arising from the base level variability which is equivalent to the term SS_ε .

4. Results

4.1 Analysis of $\hat{\sigma}_{YY}$ in data measured in horizontal directions

The results of decomposing $\hat{\sigma}_{YY}$ for two horizontal directions according to equation 13 are given in the first and second columns of Tables 3 and 4 and in Figures 7 and 8. The values of the contributions from the main factor effects and the factor interactions are similar for the two directions and thus can be discussed together. The main factor effect of grain size makes the largest contribution (~43%). The second largest contribution is from the main factor effect of bleaching (~20%). Bedding makes the smallest contribution (~9%) among the main factor effects. The quantified contribution of factor interactions plotted in Figures 7 and 8 are small compared to the main effects of grain size and bleaching. The lack of interaction can be further examined in Figure 9, 10 and 11. Figures 9 and 10 show that $\ln(k)$ generally increase with grain size regardless of bedding type or bleaching. Approximately parallel lines result, as seen, if no interaction is present. Figures 10 and 11 show that bleaching generally reduces $\ln(k)$ regardless of grain size and bedding type.

The contribution from base level variability is about 33% (Table 4). The reason behind such high contribution from base level variability has been explained by Ritzi et al. (2016). Permeability is proportional to the square of the diameter of the pore openings (e.g. Chapuis, 2004; Kamann et al., 2007). Thus, samples within a single grain size category have a wide range of permeability that varies more than an order of magnitude, as also seen in unconsolidated deposits (Soltanian and Ritzi, 2014).

Table 3: Contribution to the (co)variance from the main factors and factor interactions. The numbers in column are the values of the terms in equation 13 and sum to equal the variance.

Main Factor Effects	Contribution to (Co)Variance				
	$\ln(k_{hor_max})$	$\ln(k_{hor_min})$	$\ln(k_{vert})$	Porosity	$\ln(k_{hor_max})$ and porosity covariance
Grain Size (SSr)	1.1413	1.1361	2.5577	0.0002	0.0093
Bedding (SSo)	0.2059	0.2196	1.1497	0.0001	0.0018
Bleaching (SSj)	0.5570	0.5221	1.7542	0.0005	0.0164
Factor Interaction Effects					
Grain-Size and Bedding ($SSro$)	-0.0869	-0.1158	-0.5198	0.0000	0.0004
Grain Size and Bleaching ($SSrj$)	-0.0748	-0.0965	-0.3005	-0.0001	-0.0044
Bedding and Bleaching ($SSoj$)	0.0799	0.0765	0.5747	0.0000	0.0001
All three factors ($SSroj$)	-0.0285	-0.0059	-0.1068	0.0000	0.0005
Base-level intra-category variability not differentiated by above factors ($SS\epsilon$)	0.8481	0.8722	3.6411	0.0006	0.0154

Table 4: Percent contribution to the (co)variance from the main factors and factor interactions.

Main Factor Effects	Percent Contribution to (Co)Variance				
	$\ln(k_{hor_max})$	$\ln(k_{hor_min})$	$\ln(k_{vert})$	Porosity	$\ln(k_{hor_max})$ and porosity covariance
Grain Size (SSr)	43.20%	43.56%	29.23%	14.47%	23.61%
Bedding (SSo)	7.79%	8.42%	13.14%	7.88%	4.59%
Bleaching (SSj)	21.08%	20.02%	20.05%	35.18%	41.44%
Factor Interaction Effects					
Grain-Size and Bedding ($SSro$)	-3.29%	-4.44%	-5.94%	2.50%	0.91%
Grain Size and Bleaching ($SSrj$)	-2.83%	-3.70%	-3.43%	-5.51%	-11.18%
Bedding and Bleaching ($SSoj$)	3.02%	2.93%	6.57%	-0.84%	0.31%
All three factors ($SSroj$)	-1.08%	-0.23%	-1.22%	1.52%	1.27%
Base-level intra-category variability not differentiated by above factors ($SS\varepsilon$)	32.10%	33.44%	41.61%	44.81%	39.05%

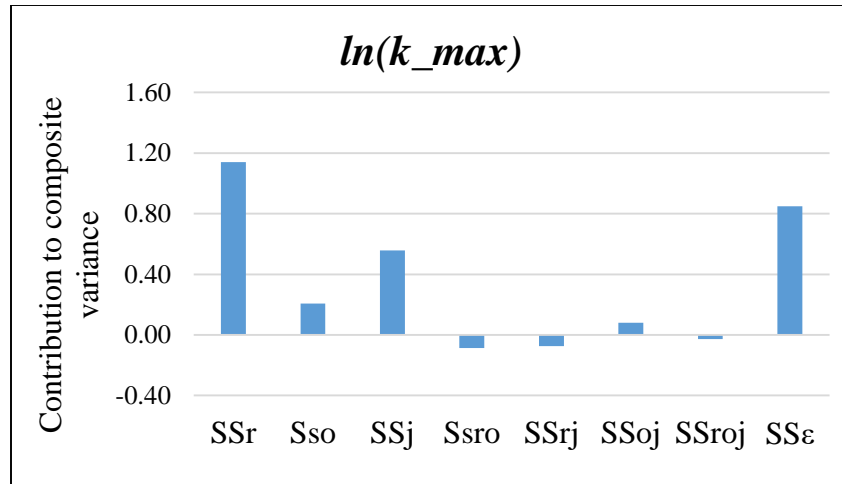


Figure 7: Contributions from the main factors and interactions to $\ln(k_{hor_max})$.

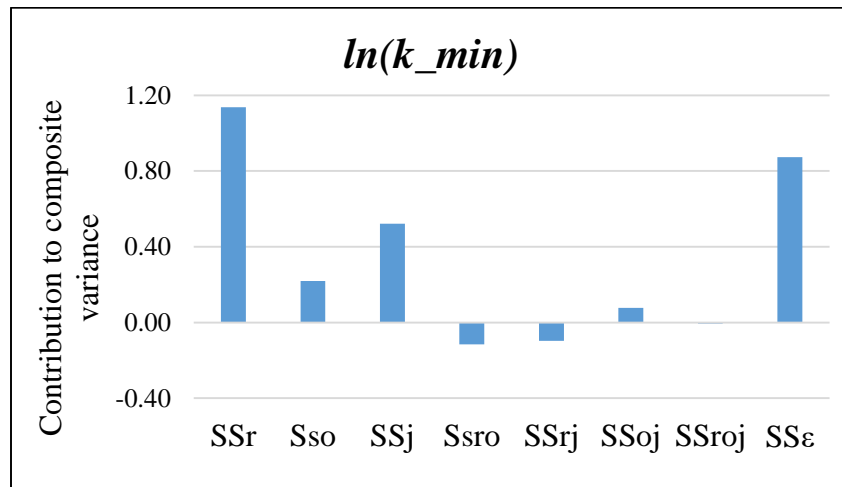


Figure 8: Contributions from the main factors and interactions to $\ln(k_{hor_min})$.

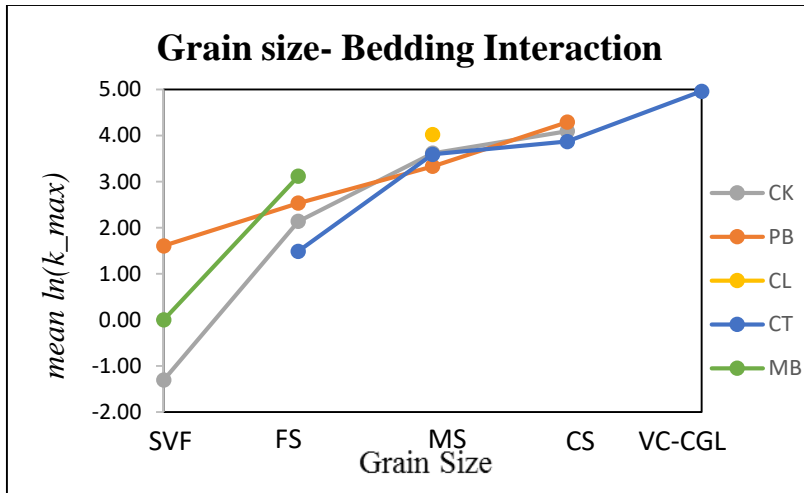


Figure 9: Grain size and bedding interaction for $\ln(k_{max})$.

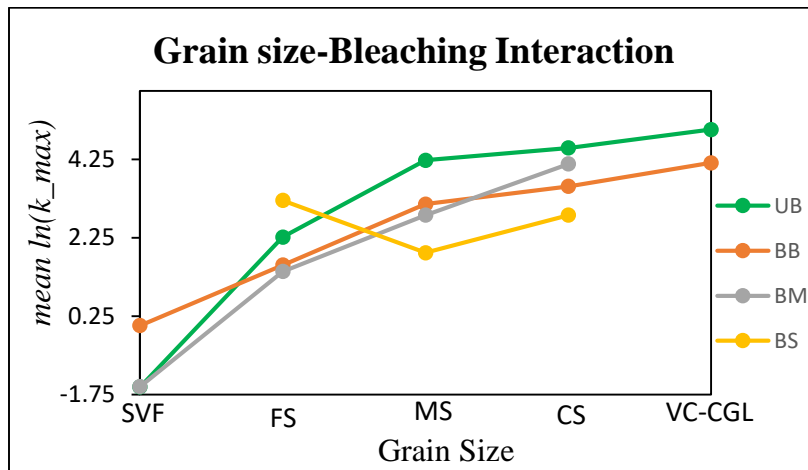


Figure 10: Grain size and bleaching interaction for $\ln(k_{max})$.

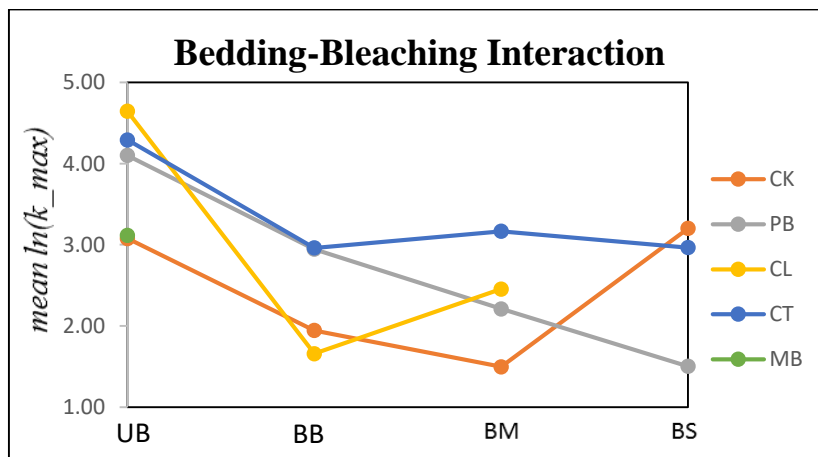


Figure 11: Bedding and bleaching interaction for $\ln(k_{max})$.

The physical meaning of these results is that the variance in $\ln(k)$ measured horizontally arises mostly from variation in grain size. Permeability increases with grain size regardless of bleaching or bedding type. Significant contribution to the variance also arises from the presence or absence of bleaching (regardless of bedding type). Differences in bedding type do not significantly contribute.

Table 5: Contribution to the (co)variance from the main factors in the hierarchical method.

Factors	Contribution to (Co)Variance				
	$\ln(k_{hor_max})$	$\ln(k_{hor_min})$	$\ln(k_{vert})$	Porosity	$\ln(k_{hor_max})$ and porosity covariance
α	1.1413	1.1361	2.5577	0.0002	0.0093
β	0.1190	0.0959	0.6299	0.0001	0.0022
χ	0.5336	0.4905	1.9216	0.0004	0.0126
ε	0.8481	0.8992	3.6412	0.0006	0.0154

Table 6: Percent contribution to the (co)variance from the main factors in the hierarchical method.

Factors	Percent Contribution to (Co)Variance				
	$\ln(k_{hor_max})$	$\ln(k_{hor_min})$	$\ln(k_{vert})$	Porosity	$\ln(k_{hor_max})$ and porosity covariance
α	43.20%	43.56%	29.23%	14.47%	23.61%
β	4.50%	3.63%	7.20%	10.38%	3.98%
χ	20.20%	18.55%	21.96%	30.34%	32.63%
ε	32.10%	34.01%	41.61%	44.81%	40.46%

Table 5 and 6 present the contributions of the terms defined in the hierarchical method of Ritzi et al. (2016). The α term represents only the grain size factor, and so row 1 in Table 5 is exactly equal to row 1 in Table 3. The β term represents the bedding main factor effect plus the grain size-bedding interaction. Because the interaction is negligible, row 2 in Tables 3 and 5 are very similar. The χ term represents the bleaching main factor effect plus grain size-bleaching interaction, the bedding-bleaching interaction and the grain size-bedding-bleaching interaction. As the interaction terms are very small, row 3 in Table 3 and 5 are similar.

4.2 Analysis of $\hat{\sigma}_{YY}$ in data measured in the vertical direction

The third column of Tables 3 and 4 and Figure 12 show the contributions from the main factor effects and the factor interactions to the sample variance of vertical permeability. The main effect of grain size makes the largest contribution (29%). The second highest contribution comes from the main effect of bleaching (20%). Bedding makes the smallest contribution (13%) among the main factor effects. Contribution from the base level variability is 42%.

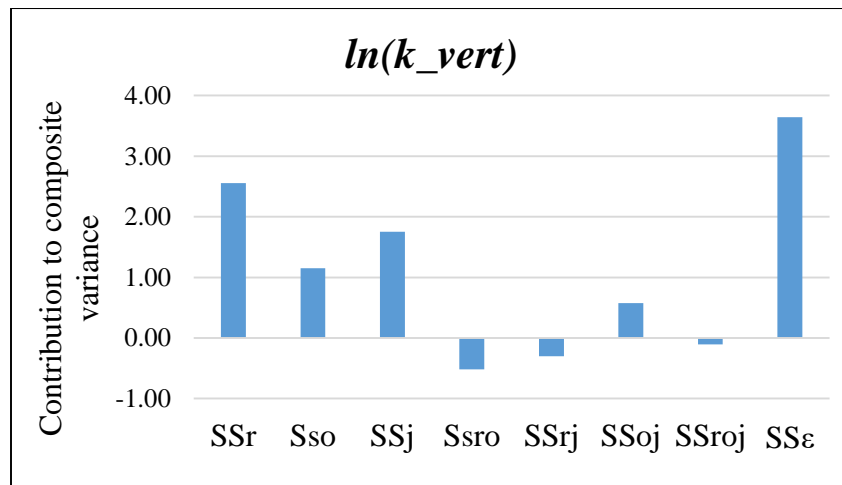


Figure 12: Contributions from the main factors and factor interactions to $\ln(k_{vert})$.

The factor interaction effects are very small and negligible as shown in Figure 12. In Figures 13 and 14 the interaction effect from the grain size and bedding, and from the grain size and bleaching factors are plotted respectively. Both plots show an increase in permeability with grain size regardless of bedding type or bleaching. Figure 15 represents factor interaction between bedding and bleaching factors. All of these three plots show generally parallel lines indicating very little to no interaction.

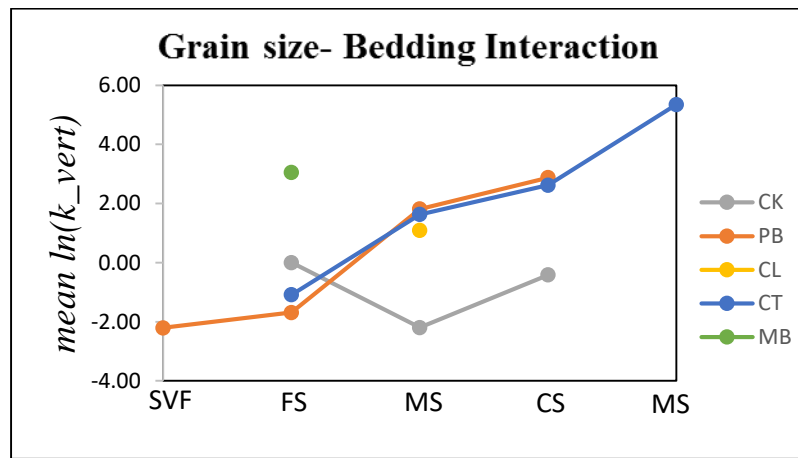


Figure 13: Grain size and bedding interaction for $\ln(k_{vert})$.

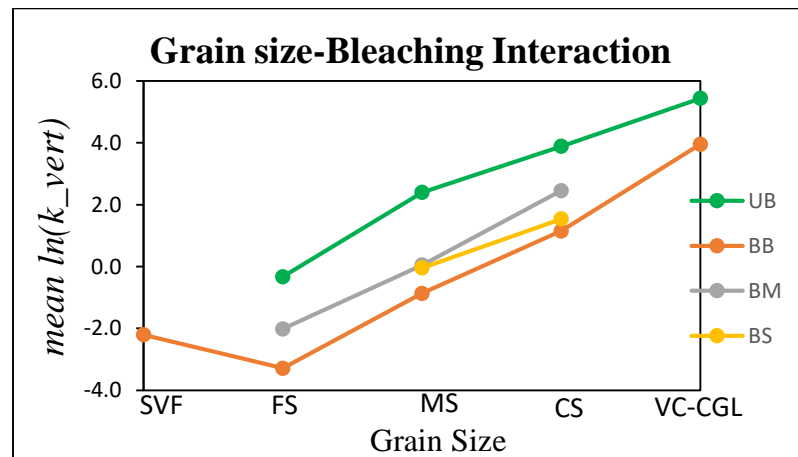


Figure 14: Grain size and bleaching interaction for $\ln(k_{vert})$.

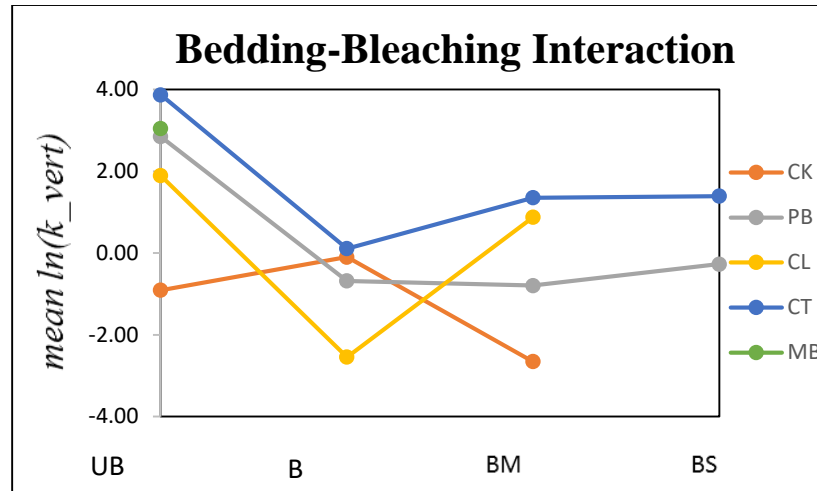


Figure 15: Bedding and bleaching interaction for $\ln(k_{\text{vert}})$.

The physical meaning of these results is that the variance in $\ln(k)$ measured vertically comes mostly from variation in grain size. Permeability increases with grain size regardless of bleaching or bedding type. Significant contribution to the variance also arises from the presence or absence of bleaching (regardless of bedding type). Differences in bedding type do not significantly contribute.

Results from the hierarchical method, presented in Tables 5 and 6 are similar to the results in Tables 3 and 4. Very small interactions from the combined factors make the main factor effects in the new method similar to the respective terms calculated in the hierarchical method.

4.3 Analysis of $\hat{\sigma}_{\phi\phi}$

The fourth column of Tables 3 and 4 and Figure 16 represent the results for porosity. The main effect from the bleaching category makes the largest contribution (35%) to the sample variance of porosity. The second highest contribution comes from the main effect of grain size (14%). Bedding makes the lowest contribution among the main factors (8%). Contribution arising from the base level variability is very high (45%).

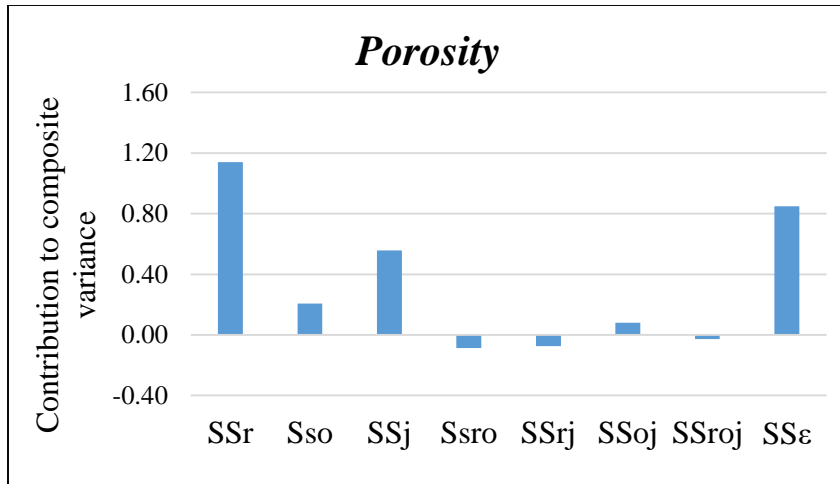


Figure 16: Contributions from the main factors and factor interactions to porosity.

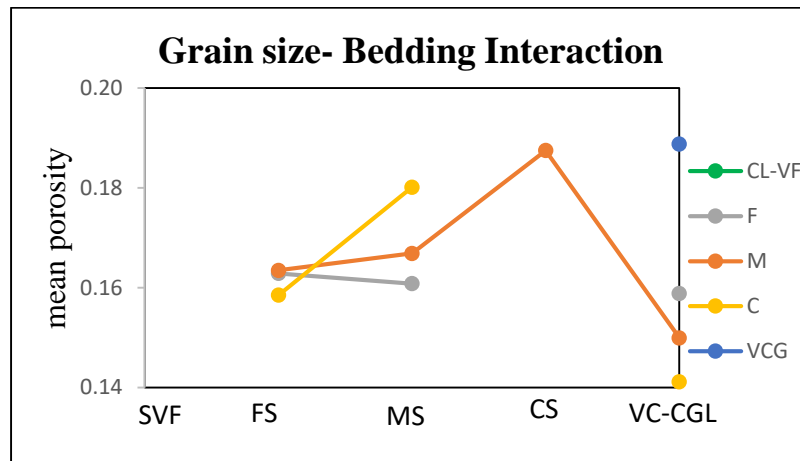


Figure 17: Grain size and bedding interaction for porosity.

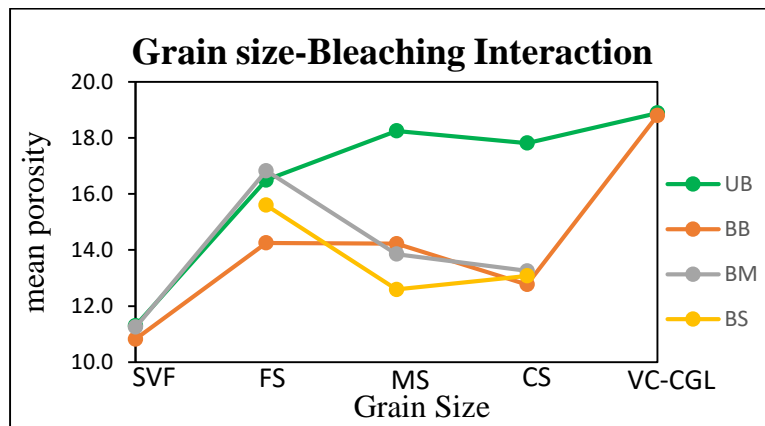


Figure 18: Grain size and bleaching interaction for porosity.

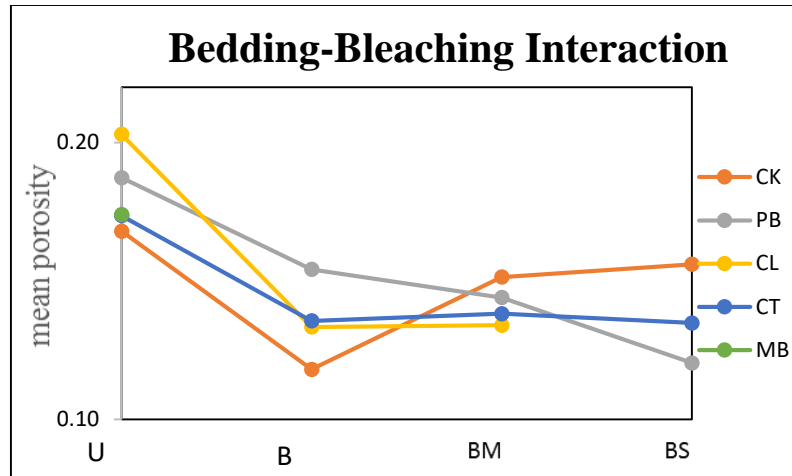


Figure 19: Bedding and bleaching interaction for porosity.

Contributions from the factor interactions are very small. The plots in Figures 17, 18 and 19 represent all possible two-way factor interactions: grain size and bedding, grain size and bleaching, and bedding and bleaching. The bedding-bleaching (Fig 19) and the grain size-bleaching (Fig 17) interaction plots show that bleached samples generally have lower ϕ regardless of grain size or bedding type. Tables 5 and 6 represent similar results for porosity from the hierarchical method, which are similar because of the very small interaction effects from the combined factors.

Porosity is an absolute rather than relative measure of void space and there is less relation to absolute pore or grain size compared to Y . It is more related to the degree of sorting and packing of fine grains into coarse grains. Thus, the main factor effect of grain size contributes less to ϕ than to Y .

4.4 Analysis of $\hat{\sigma}_{Y\phi}$

The fifth column of Tables 1 and 2 and Figure 20 represent the contribution of factors to the sample covariance of horizontal intrinsic permeability (max) and porosity. These two attributes are very weakly correlated. The sample point covariance between these two attributes is 0.039 and the correlation coefficient (R value) is 0.43.

Figure 20 shows that the weak correlation between Y and ϕ is mostly from the main factor effect of bleaching. Grain size also contributes to the correlation significantly. Contribution from the bedding type is very small.

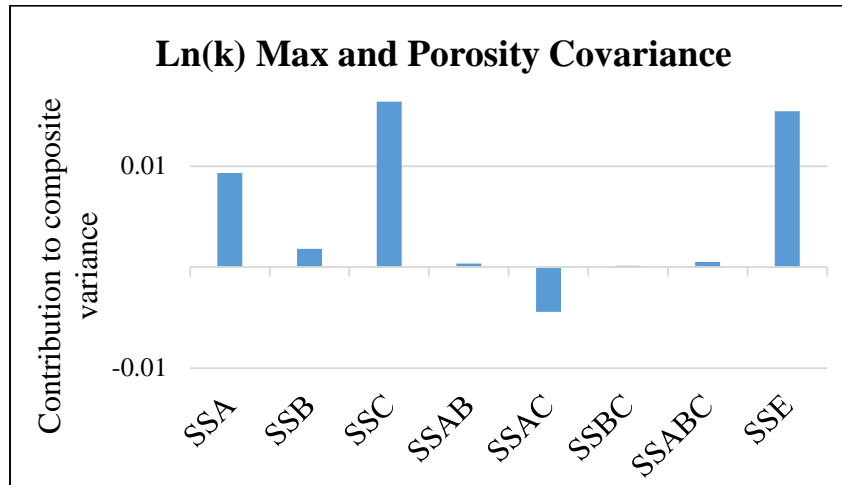


Figure 20: Contributions from the main factors and interactions to $\ln(k)$ & porosity covariance.

5. Conclusions

The analysis quantified the percent contribution of three factors (grain size, bleaching and bedding) representing sedimentary textures and structures of the reservoir rock to the sample variance of two petro-physical properties, i.e. intrinsic permeability and porosity, and to their covariance. Grain size and bleaching are the two most important factors. The main factor effect from grain size (differences between SVF, FS, MS, CS and VC-CGL) is the largest contributor to the sample variance of intrinsic permeability measured in both horizontal and vertical directions. The main factor effect of bleaching (differences between UB, BS, BM and BB) is the second largest contributor to permeability. Bleaching also mostly explains porosity and the weak permeability-porosity correlation.

The main effect of the bedding factor with the newly defined categories (differences in CK, PB, CL, CT and MB) contributes little to the sample variance or covariance of permeability and porosity. This conclusion is consistent with Ritzi et al. (2016). Although bedding does not contribute significantly to the sample variance, the bedding types correspond to geobodies with specific geometries and juxtapositioning and thus are relevant to building deposition-based geocellular models for the reservoir (Gershenzen et al., 2015).

Interaction effects were quantified and shown to be negligible in this analysis. The conclusions in this study are consistent with those of Ritzi et al. (2016) because factor interactions were indeed negligible as was assumed by Ritzi et al. (2016).

This study explains very clearly how a number of factors can be used in understanding the sample variance and covariance of permeability and porosity. The application of this method could be used to analyze the sample variance and covariance of other physical

properties, for example, the Young’s modulus, the Poisson ratio or the shear modulus, which need to be better understood to interpret microseismicity at the site.

Facies classifications are not unique (Ritzi et al., 2016). Ritzi et al. (2016) proposed a parsimonious 4-facies conceptual model to represent the variability in the attributes given in Table 7 and Figure 24. Since bedding type and vertical position were shown not to be important factors, they were not included. The goal was to minimize the number of facies needed to represent the variability in the attributes. Grain size and bleaching were the two factors that were included in the model. The five grain size categories were combined into two groups: fine grained and coarse grained. The four bleaching categories were combined into two groups: unbleached and bleached. The results of the analysis of variance here are consistent with Ritzi et al. (2016). Therefore, these results also support the parsimonious 4-facies conceptual model proposed by Ritzi et al. (2016).

Table 7: Example of a parsimonious classification with four facies (Ritzi et al., 2016).

Textural facies category	% of reservoir	Geom. Mean (mD)	CV	Porosity
Unbleached finer-grained	8%	10	1	20%
Unbleached coarser-grained	32%	100	1	20%
Bleached finer-grained	12%	2.5	2	15%
Bleached coarser-grained	48%	25	2	15%

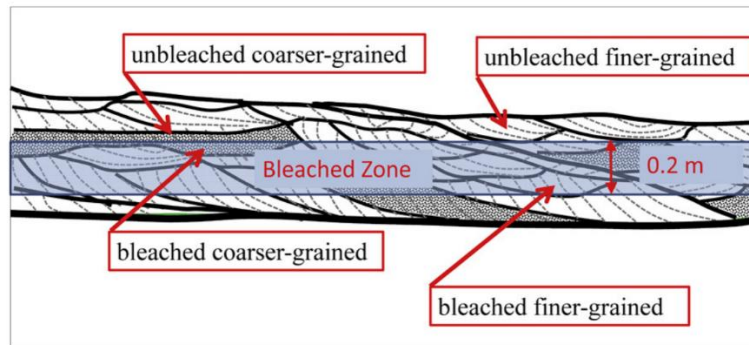


Figure 24: Conceptual model for four textural facies as assigned within depositional Units including cross-sets and cross bar fills (Ritzi et al., 2016).

References

- Chapuis, R.P., Aubertin, M., 2003. *On the use of the Kozeny-Carmen equation to predict the hydraulic conductivity of soils*. *Can. Geotechnol. J.* 40 (3), 616–628.
- Dixon, S.A., D.M. Summers, and R.C. Surdam, 1989. *Diagenesis and preservation of porosity in Norphlet Formation (Upper Jurassic), southern Alabama*: AAPG Bulletin, v. 73, p. 707–728.
- Finley, R.J., 2014. *An overview of the Illinois Basin—Decatur Project*. *Greenhouse Gas Sci. Technol.* 4, doi. 10.1002/ghg.1433.
- Freiburg, J.T., Morse, D.G., Leetaru, H.E., Hoss, R.P., Yan, Q., 2014. *A Depositional and Diagenetic Characterization of the Mt. Simon Sandstone at the Illinois Basin-Decatur Project Carbon Capture and Storage Site*. Circular 583, Illinois State Geological Survey, Decatur, Illinois, USA, 53 p.
- Gershenson, N.I., Soltanian, M.R., Ritzi, R.W., Dominic, D., Mehnert, E., Okwen, R., 2015b. *Influence of small-scale, fluvial, sedimentary architecture on CO₂ trapping processes in deep brine reservoirs*. *Water Resour. Res.* 15 (10), doi. 10.1130/GES01115.1.
- Kutner, M., Nachtsheim, C., Neter, J., Li, W., 2004. *Applied linear statistical models*. McGraw-Hill Irwin, p. 1396.
- Kamann, P.J., Ritzi, R.W., Dominic, D.F., Conrad, C.M., 2007. *Porosity and permeability in sediment mixtures*. *Ground Water*. v. 45, Issue 4, p. 429-438, doi. 10.1111/j.1745-6584.2007.00313.x.
- Levandowski, D.W., M.E. Kaley, S.R. Silverman, and R.G. Smalley, 1973. *Cementation in Lyons Sandstone and its role in oil accumulation, Denver Basin, Colorado*: AAPG Bulletin, v. 57, p. 2217–2254.

McKee, E. and Weir, G.W. (1953), *Terminology for Stratification and Cross-Stratification in Sedimentary Rocks*. *Geological Society of America Bulletin*, v. 64, p. 381-390, doi. 10.1130/0016-7606(1953)64[381:TFSACI]2.0.CO;2.

Moulton, G.F., 1926. *Some features of redbed bleaching*: AAPG Bulletin, v. 10, p. 304–311

Todd, T.W., 1963. *Post-depositional history of Tensleep Sandstone (Pennsylvanian), Big Horn Basin, Wyoming*: AAPG Bulletin, v. 47, p. 599–616.

Parry, W.T., A.C. Marjorie, and B. Beitler, 2004. *Chemical Bleaching Indicates Episodes of Fluid Flow in Deformation Bands in Sandstone*: AAPG Bulletin, v. 88, no. 2, p. 1756–1792.

Ramanathan, R., Guin, A., Ritzi Jr., R.W., Dominic, D.F., Freedman, V.L., Scheibe, T.D., Lunt, I.A., 2010. *Simulating the heterogeneity in braided channel belt deposits: I. A geometric-based methodology and code*. *Water Resour. Res.* 46, W04515, doi. 10.1029/2009wr008111.

Ritzi, R.W., Freiburg J.T., Webb, N.D., 2016. *Understanding the (co)variance in petrophysical properties of CO2 reservoirs comprising sedimentary architecture*. *Int. J. Greenhouse Gas Control* 51

Roden, E.E., 2008. *Microbiological Controls on Geochemical Kinetics 2: Case Study on Microbial Oxidation of Metal Sulfide Minerals and Future Prospects*, in S.L. Brantley, J. Kubicki, and A.F. White, eds., *Kinetics of Water–Rock Interactions*: New York, Springer, p. 417–467.

Soltanian, M.R., Ritzi, R.W., 2014. *A New Method for Analysis of Variance of the Hydraulic and Reactive Attributes of Aquifers as Linked to Hierarchical and Multi-scaled Sedimentary Architecture*. *Water Resour. V.* 50, Issue 12, p. 9766-9776, doi. 10.1002/2014WR015468.

Surdam, R.C., T.L. Dunn, H.P. Heasler, and D.B. MacGowan, 1989. *Porosity Evolution in Sandstones/Shale Systems*, in I.E. Hutcheon, ed., *Short Course on Burial Diagenesis*: Montreal, Mineralogical Association of Canada, p. 61–133.